Comprehensive Hydrodynamic Analysis of Oscillating Flapping Mechanism for Enhanced Wave Energy Converter Technology

Fitri Wahyuni[1], Rizki Aldi Anggara[1], James Julian[1*], Riki Hendra Purba[1]

[1]Teknik Mesin, Fakultas Teknik, Universitas Pembangunan Nasional Veteran Jakarta
Jalan RS. Fatmawati Raya, Pondok Labu, South Jakarta City, Jakarta, Indonesia
**Corresponding author*: zames@upnvj.ac.id

Abstract

The comprehensive utilization of renewable energy stands as a national priority within Indonesia's strategic framework aimed at achieving the net zero emissions target by 2060. Indonesia, a nation in which nearly 70% of its territory is comprised of oceans, possesses significant potential in wave energy as a renewable energy source. This sector presents promising opportunities for development and investment. This study focuses on the three-dimensional hydrodynamic study of Wave Energy Converter (WEC) technology based on oscillating flapping through a numerical approach. The findings of the characteristic test demonstrate that the oscillating flapping device exhibits a response characterized by a deviation in the oscillating tilt angle. The direct impact of ocean waves causes the flap to shift from its equilibrium position and continuously move back and forth with a particular frequency. The dynamics working on this device show a correlation between wave input and the response that occurs. The response parameters, including maximum angular deviation, average speed, and torque, have a similar trend to changes in wave period. The influence of ocean wave activity is observed to increase within the low wave period zone up to a designated period threshold. Overall, the oscillating flapping device demonstrates enhanced performance in low wave conditions. The average maximum output power is capable of reaching 1.5 Watts on A1, 3.5 Watts on A2, and 4.5 Watts on A3.

Keywords**:** *net zero emissions, oscillating flapping, ocean waves, renewable energy, wave energy converter*.

1. Introduction

The issues of pollution and carbon emissions have emerged as prominent global concerns in recent times. Climate change, energy crisis, damage, and environmental pollution are projected to have a significant impact in the long term [1]. In addition, health issues have increased in direct proportion to problems that occur in the environment [2]. Dependence on fossil fuels as environmentally unfriendly energy is one of the main factors responsible for the problems that occur [3]. As the country with the largest population in Southeast Asia, Indonesia has the highest energy consumption, with a record of 40% of total energy consumption in the ASEAN region [4]. However, energy dependence dominated by fossil fuels makes Indonesia one of the countries responsible for the climate impacts that occur. Therefore, various countries have contributed to compiling regulations that focus on renewable energy transitions as a strategic step in overcoming the growing problem issues.

The comprehensive utilization of renewable energy is a national priority in Indonesia's strategy to commit to the net zero emissions target by 2060 [5, 6]. This obligation is supported by state regulations in Government Regulation No. 79 of 2014 regarding national energy policy [5]. In addition, Indonesia and 40 other countries signed the Global Goal to Clean Power Transition declaration at the 26th Conference of the Parties (COP26) [4]. Indonesia is an archipelagic country, with almost 70% of its territory comprising oceans [7]. This geographical condition provides a decisive advantage as a country with a sea that has abundant renewable energy resources. Ocean wave energy is one of Indonesia's renewable energy sources with promising prospects. Indonesia's ocean wave energy potential in Southeast Asia has reached the highest predicate of 510 GW [8].

Over the past few decades, the prospect of ocean wave energy has attracted

DOI: http://dx.doi.org/10.24127/trb.v14i1.3786
Received November 13, 2024; Received in revised form June 29, 2025; Accepted June 29, 2025
Available online June 30, 2025

researchers to developing Wave Energy Converter (WEC) technology. WEC is a wave energy converter technology that utilizes mechanical work to convert electrical energy [9]. In general, the development of WEC technology covers broad aspects in diverse types of WEC technology, including Oscillating Water Coulomb (OWC), Overtopping, Point Absorber, Oscillating Wave Surge Converter (OWSC), and others [10–13]. Thus far, OWSC with the oscillating flapping type is one of the technologies with a record with a high level of performance compared to other types [14]. In addition, the track record of research development of this technology shows its potential. Oyster and Wave-Roller technologies are examples of successful OWSC technology developments to the commercial stage [15, 16].

In the research scale, the development aspects of OWSC technology contain characteristic studies, performance testing, and optimization. OWSC characteristic studies focus on characterizing the mechanism of the hydrodynamic phenomena that occur [17]. Related research studies the characteristics of OWSC with the intent of understanding the interactions that occur in OWSC technology with sea waves [18]. Several studies include research that focuses on fundamental and theoretical problems, such as model concepts, theoretical modeling, and hydrodynamic phenomena (viscosity and slamming effects) [19–23]. In addition, testing the performance of power capture on OWSC technology is followed by optimization. Some studies focus on hydrodynamic performance and efficiency in optimizing the studied model. Several related studies expose vital parameters that are crucial to the performance of OWSC technology, including load damping, geometry, plate configuration, and resonant adjustment [24–28].

Based on the literature study results, the study of OWSC technology is generally a two-dimensional concept, and the influence of the width of the converter object is ignored. The analysis process of the phenomena that occur is limited and significantly impacts accuracy, so experimental testing is needed to support the validity of the data obtained. However, high funding is needed to obtain supporting laboratory facilities in the experimental setup. Therefore, this study investigates the three-dimensional hydrodynamic characteristics of oscillating flapping-based wave energy converter (WEC) technology, employing a numerical approach complemented by a validation process. This methodology ensures the integrity and currency of the data, facilitating a comprehensive analysis of the subject matter. Considering that Indonesia has promising potential for ocean wave energy sources, the development of WEC technology in Indonesia has attracted less attention and has yet to show a significant trend [8]. Therefore, this study can provide an overview of the potential prospects of OWSC technology as an environmentally friendly and sustainable renewable energy technology.

2. Methodology

2.1 Oscillating flapping

Oscillating flapping is one type of WEC technology that utilizes a hinged plate/flap object as a direct wave energy converter [29]. This technology is part of the OWSC classification using an inverted pendulum mechanism to convert wave energy into oscillatory motion. This study focuses on oscillating flapping as a primary research subject to examine the associated hydrodynamic phenomena and to assess the performance of the device under varying wave conditions. To minimize the complexity of testing, a simple form of the OWSC model investigated is arranged through a scaling model. Specifically, the design and parameters of the oscillating flapping model are illustrated in Figure 1 and Table 1.

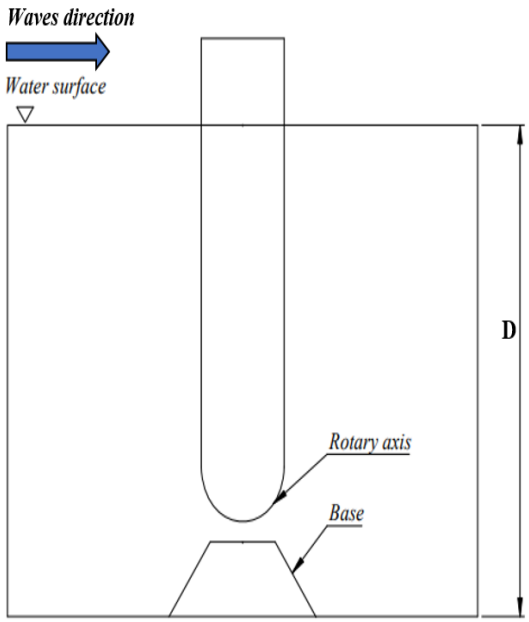

(a) Schematic OWSC

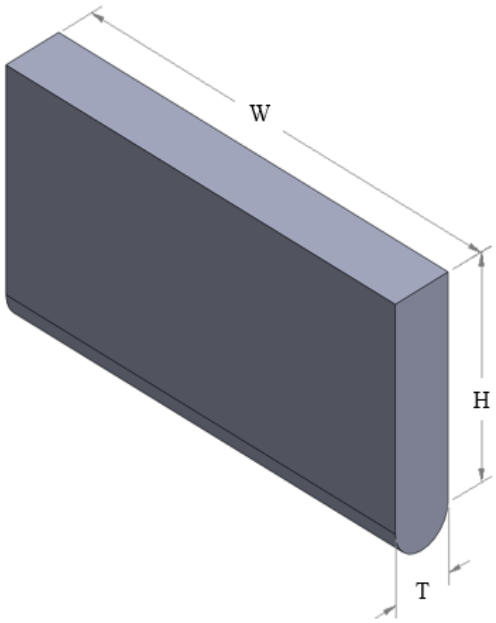

(b) OWSC dimensions

Figure 1. Oscillating flapping

Table 1. Design parameters

No.	Parameter	Value
1	Scaling factor	74^{th}
2	W (m)	0.35
3	H (m)	0.168
4	T (m)	0.047
5	D (m)	0.165
6	Mass (kg)	0.681

2.2 Numerical method

In facilitating the testing process, numerical calculations are employed as a methodological approach to addressing the examined cases. The interaction between sea waves and the oscillating flapping device is described using the Boundary Element Method (BEM). This approach utilizes numerical techniques involving potential flow involving the Laplace and Bernoulli equations to determine the forces and torques acting on the flap [17]. This method assumes incompressible and inviscid fluid flow conditions. Based on the potential flow theory, the wave excitation force is set in Equation (1). Specifically, the computation process involves two schemes: frequency and time domains. In the frequency domain scheme, the hydrodynamic parameters acting on the oscillating flapping are calculated using Equation (2), which includes nonlinear hydrostatic and Froude-Krylov force. Furthermore, the flap response as a mechanical system is reviewed in the time domain scope as the output set in Equation (3) is included with the device performance parameters [14, 30].

$$\nabla^2\phi(x,y,z,t) = \phi_I(x,y,z,t) + \phi_D(x,y,z,t) + \phi_R(x,y,z,t) = a_W\varphi(x,y,z)e^{-i\omega t} \quad (1)$$

$$\left[-\omega^2(M_s + M_a(\omega)) - i\omega C(\omega) + K\right] X(\omega) = F(\omega) \quad (2)$$

$$M\ddot{X}(t) + C\dot{X}(t) + KX(t) + C_h\dot{X}(t) = F(t) \quad (3)$$

2.3 Boundary condition

This study examined the oscillating flapping device in two areas: characteristics and hydrodynamic performance. A study was conducted to analyze the response resulting from the interaction between an oscillating flapping device and ocean waves. As an electrical converter technology, the oscillating flapping performance was tested based on hydrodynamic performance. The power capture capability of the device was investigated in each wave variation. In addition, the efficiency of the oscillating

flapping device was evaluated. In the process of analyzing the hydrodynamic performance of the oscillating flapping device, several equations that regulate the mechanical power of the device and ocean wave propagation, as well as the capture width ratio, are presented in Equations (4), (5), and (6). Specifically, the variations in the wave input parameters are described in Table 2.

$$P_{OWSC} = \left|\tau(t) \times \omega(t)\right| \quad (4)$$

$$P_w = \frac{1}{2}\rho g A^2 C_g \quad (5)$$

$$CWR = \frac{P_{OWSC}}{P_w \times Width} \quad (6)$$

Table 2. Ocean wave parameters

No	Amplitudo (m)			Periode
	A1	A2	A3	(s)
1	0.03	0.054	0.06	0.810
2	0.03	0.054	0.06	0.957
3	0.03	0.054	0.06	1.104
4	0.03	0.054	0.06	1.251
5	0.03	0.054	0.06	1.398
6	0.03	0.054	0.06	1.545
7	0.03	0.054	0.06	1.693
8	0.03	0.054	0.06	1.840
9	0.03	0.054	0.06	1.987
10	0.03	0.054	0.06	2.134

2.4 Mesh independence test

A mesh independence test is performed to identify the mesh quality used in the numerical calculation process. This assessment represents a pivotal phase in the numerical methodology, as it significantly influences the precision and reliability of the resultant data. Therefore, the mesh independence test is conducted based on the method applied in Roache's research [31]. This study classifies mesh categories based on the number of elements: fine, medium, and coarse. The number of elements in each mesh category includes 24930, 12643, and 6308.

The Root Mean Square (RMS) value of the oscillatory response on the flap, with wave specifications defined by parameters A = 0.054 and T = 1.398, is employed as a representative test sample. This value is incorporated across multiple mesh categories by Equation (7). Each mesh category is identified through the grid refinement ratio calculated in Equation (8). Furthermore, the order value is determined through Equation (9). In testing the error value of each mesh category, the Grid Convergence Index (GCI) is used, which is calculated in Equations (10) and (11). GCI is divided into two categories: GCI_{fine} is the error value between fine mesh and medium mesh, and GCI_{coarse} is the error value between medium mesh and coarse mesh. The GCI calculation must be conducted within the convergence area to reflect the actual error values for each mesh accurately. Therefore, the actual value of the mesh independence test can be obtained in Equation (14). The results of the mesh independence test can be seen in Table 3. The test results analysis indicates that the fine mesh configuration demonstrates a high degree of accuracy, evidenced by its minimal error value. Consequently, the fine mesh has been designated as the preferred setup for the study.

$$RMS = \sqrt{\frac{1}{n}\sum_i x^2{}_i} \quad (7)$$

$$r = \frac{h_2}{h_1} \quad (8)$$

$$\bar{p} = \frac{\ln\left(\frac{f_3 - f_2}{f_2 - f_1}\right)}{\ln(r)} \quad (9)$$

$$GCI_{fine} = \frac{F_s \left|\in\right|}{\left(r^{\bar{p}} - 1\right)} \quad (10)$$

$$GCI_{coarse} = \frac{F_s \left|\in\right| r^{\bar{p}}}{\left(r^{\bar{p}} - 1\right)} \quad (11)$$

$$\in = \frac{f_{n+1} - f_n}{f_n} \quad (12)$$

$$\frac{GCI_{coarse}}{GCI_{fine} r^{\bar{p}}} \approx 1 \quad (13)$$

$$f\mathrm{r}_{h=0} = f_1 + \frac{(f_1 - f_2)}{\left(r^{\bar{p}} - 1\right)} \quad (14)$$

Tabel 3. Mesh independence test results

Mesh	*Fine*	*Medium*	*Coarse*
RMS	50,05052374	47,57824319	4062833194
	1,491152093		
r	2		
GCI_{fine}	3,586%		
GCI_{coarse}	10,0816%		
$\frac{GCI_{coarse}}{GCI_{fine}r^{p}}$	1		
$f_{rh} = 0$	51,41556956		
Error	2,65493 %	7,46335 %	20,98049%

3. Results and Discussion

3.1 Validation

In the numerical approach, it is imperative to undertake validation to ascertain the degree of actualization of the derived data results. The validation process is carried out by comparing the computational data with experimental data. This study involves experimental data through research conducted by Wei on testing the oscillating wave surge converter (OWSC) device [23]. The motion response of the OWSC device is used to compare data.

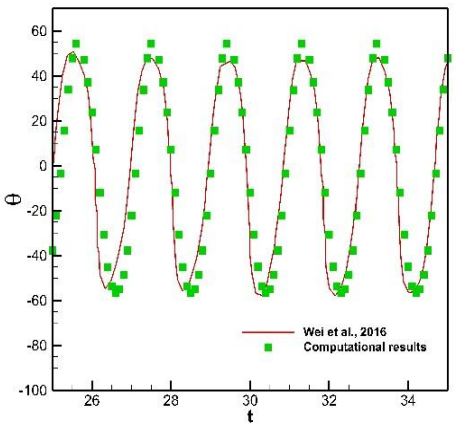

Figure 2. OWSC motion response (°)

The motion response data of the OWSC device was taken at specific sea waves A = 0.1m and T = 1.9s. The results of the comparison of motion response data on the OWSC device can be seen in Figure 2. Based on the results of the numerical approach, comparing the flap response shows similarities with the experimental results at frequency and phase angle. However, there are slight differences in predicting the maximum deviation response on the flap due to the limitations of the approach method. However, the numerical calculation data is still able to maintain a trend and similarity of results that are significant with the experimental data.

3.2 Analysis

Figure 3 shows the motion response of the oscillating flapping device to the incident of sea waves. In this context, the flap functions as a device specifically designed to directly absorb the impact of sea waves and convert this kinetic energy into electrical energy. The flap connected to the hinge causes a working response through angular displacement. Continuously, the angle experiences an oscillating deviation from the equilibrium position. This condition is caused by the motion of sea wave particles forming an ellipse and oscillating as a characteristic of waves with a seabed effect.

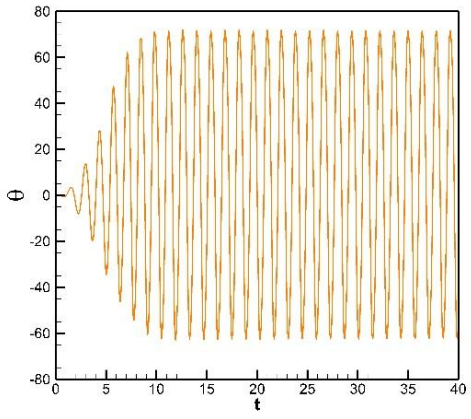

Figure 3. Oscillating flapping device motion response (°)

As an object with inertia, the dynamics working on the oscillating

flapping device are reviewed further in the characterization. Figure 4 explicitly shows the correlation between the device's response to the occurring dynamics. The angular velocity and torque generated at the hinge describe each condition/phenomenon that occurs on the flap at each angular position. Based on the test results, the torque working on the hinge has a phase angle relationship of up to 180°. Therefore, both parameters show opposite vector directions. Furthermore, the angular velocity and torque parameters at the hinge represent critical variables that significantly influence the mechanical output power generated by the oscillating flapping device. It can be seen that the output power has an absolute relationship that is directly proportional to the angular velocity and torque components so that the product results show a positive value followed by an increase in frequency on the curve.

In addition, a more in-depth review of the hydrodynamic performance of the oscillating flapping device is conducted. Further analysis of the dynamics of the response in the device is discussed against variations of different types of waves. As seen in Figure 5, the maximum angular deviation, average angular velocity, and torque curves show a similar trend. The maximum deviation is observed to increase with an extension in the wave period, followed by an increase in average angular velocity and torque components until a defined maximum threshold is achieved. When the oscillating flapping is tested with wave type A1, it can be seen that the maximum deviation occurs up to 50° at period T = 1.6s. As the wave period increases, the influence of incoming sea waves on the resulting deviations becomes less significant. The flap shows more dominant characteristics at short wave periods, where the resulting oscillation frequency is more extreme. This condition is supported when the amplitude of sea waves increases (in wave variations A2 and A3), where there is a shift in the maximum point of the dynamic response experienced by the device towards a shorter wave period up to T = 1.2s.

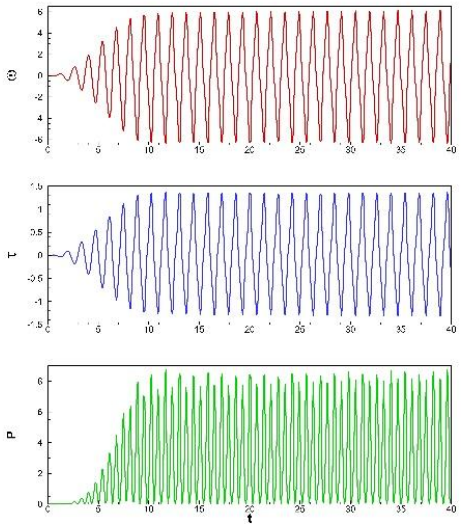

Figure 4. Hydrodynamic characteristic parameters of the oscillating flapping device, including angular velocity (rad/s), torque (Nm), and hydrodynamic power (Watt)

The characteristic behavior of the oscillating flapping device is directly proportional to the average output power produced. Figure 6 compares the device's output power to the propagation power of ocean waves. The propagation power of ocean waves shows a constructive trend, increasing consistently with extended wave periods. This is assessed by the ability of the wave to maintain the energy carried in a unit of time. In the oscillating flapping device, it has been observed that it can sustain operation for a maximum wave period of T = 1.6 s, achieving a peak power output of approximately 1.5 Watts in the A1 variation. The increase in wave amplitude is directly proportional to the increase in output power, where the A2 variation has an average maximum output power of 3.5 Watts and 4.5 Watts in the A3 wave variation. However, there is a shift in the wave period (T = 1.2s in the A2 and A3 wave variations) at maximum power. The capacity of the device to absorb wave energy exhibits a diminishing efficiency at elevated amplitudes, ultimately leading to a degradation in performance as wave periods increase.

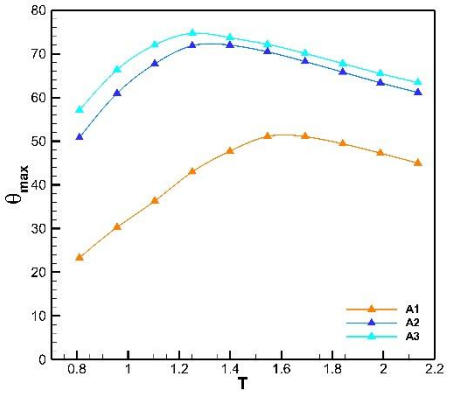

(a) Angular deviation maximum (°)

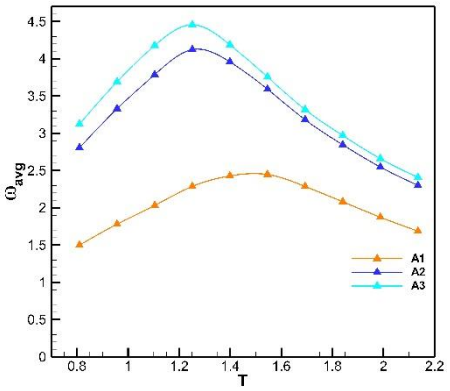

(b) Average angular velocity

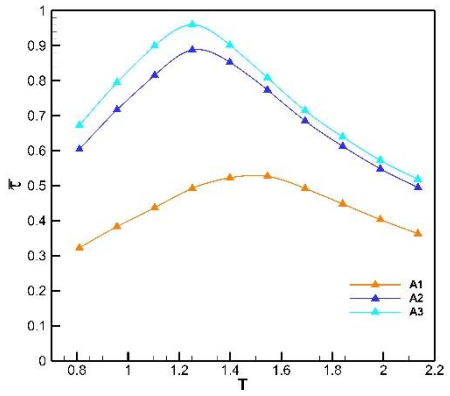

(c) Average torque

Figure 5. Performance of the oscillating flapping device against variations in waves period

More specifically, a focused examination of the efficiency of the oscillating flapping device's performance is conducted. Capture width ratio (CWR) is defined as the ratio of the power capture capability of the device to the propagation power of ocean waves. The test results indicate that the oscillating flapping device exhibits high efficiency across a range of wave variations, particularly at low periods. It can be seen in Figure 7 that there is no significant difference in CWR efficiency in every wave variation with a low period.

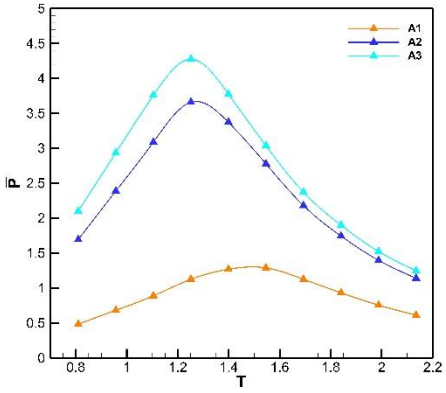

(a) Average power output (Watt)

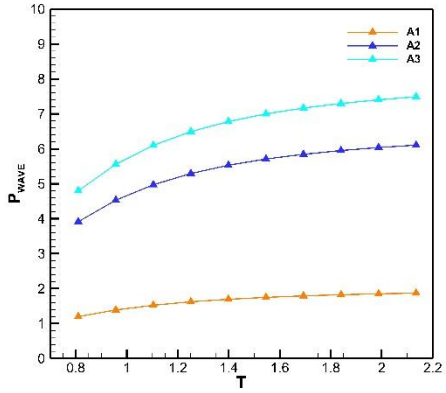

(b) power of wave propagation (Watt)

Figure 6. Hydrodynamic power of the oscillating flapping device against the propagation power of sea waves

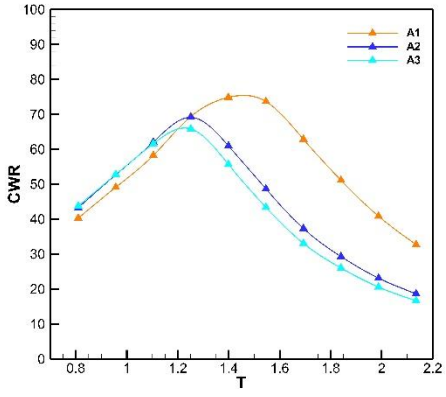

Figure 7. Capture width ratio (CWR)

However, there is a difference in the maximum point at a higher wave variation,

whereas, at the period T = 1.2s, the maximum efficiency is only able to reach 70%. At lower wave height, the performance of the device increases, and the maximum efficiency of the device can be achieved up to 75% with a broader period interval shift at T = 1.4s. This device tends to operate effectively, especially when the wave period is shorter. Therefore, the flapping mechanism that utilizes direct wave impacts is more dominant in absorbing kinetic energy. While there is no statistically significant difference observed in the maximum captured wave energy results, the shift of the peak response to a reduced period in the context of increased wave incidence highlights a constriction in the operational performance range of the oscillating floating device. This narrowing effect may have implications for the device's efficacy under varying wave conditions.

4. Conclusion

The hydrodynamic analysis of a three-dimensional model of an oscillating flapping device was conducted using numerical methods to investigate the hydrodynamic characteristics and performance metrics associated with its operation. The test was carried out under different wave variation conditions, followed by validation of the numerical setup to obtain a comprehensive actualization and discussion. In the characteristic test, the study demonstrated that the oscillating flapping device exhibited a notable response, characterized by a deviation in the oscillating tilt angle. The direct impact of sea waves causes the flap to shift from its equilibrium position and oscillate back and forth at a specific frequency. The dynamics that work on this device show a correlation between wave input and the response that occurs.

Moreover, understanding the impact of wave conditions offers valuable insights into the response characteristics of the oscillating flapping device. The test results show that the response parameters, including maximum angular deviation, average angular velocity, and torque, have a similar trend to changes in wave period. The maximum deviation increases with the wave period until it reaches its maximum point. Once the wave period exceeds a certain point, the impact of sea waves tends to diminish, leading to a reduction in the working response. Overall, this device shows a more dominant performance in low-wave periods. The increase in sea wave amplitude is directly related to the increase in output power. The average maximum output power can reach 1.5 Watts at A1, 3.5 Watts at A2, and 4.5 Watts at A3. However, the maximum power generated is limited to short wave periods. The efficiency of the device, reviewed through the capture width ratio (CWR), is relatively stable in various types of waves. This condition indicates that the device can function effectively in every wave variation. Along with the increase in wave amplitude, there is a shift in the maximum point to a lower wave period, limiting the device's ability to absorb energy at more extended wave periods. Therefore, it is recommended that the wave period and amplitude be considered as the key to determining the location and operation of the oscillating flapping device to achieve optimal performance.

References

[1] Zubaydah A, Sabilah AZ, Sari DP, et al. Mengurangi Emisi: Mendorong Transisi Ke Energi Bersih Untuk Mengatasi Polusi Udara. *Biochephy: Journal of Science Education* 2024; 4: 11–21.

[2] Hidayat A. Dampak Polusi Udara pada Kesehatan.

[3] Setyono AE, Kiono BFT. Dari energi fosil menuju energi terbarukan: potret kondisi minyak dan gas bumi Indonesia tahun 2020–2050. *Jurnal Energi Baru Dan Terbarukan* 2021; 2: 154–162.

[4] Prasodjo H. Green diplomacy as an effort by the Indonesian government in Realizing Net Zero Emission (NZE) in the year 2060. In:

Environmental Issues and Social Inclusion in a Sustainable Era. Routledge, 2023, pp. 184–190.
[5] Zahira NP, Fadillah DP. Pemerintah Indonesia menuju target net zero emission (nze) tahun 2060 dengan variable renewable energy (vre) di Indonesia. *Jurnal Ilmu Sosial* 2022; 2: 114–119.
[6] Paundra F, Nurdin A. Study Of The Potential And Development Of Renewable Energy Power In Indonesia: A Review. *Steam Engineering* 2022; 3: 62–72.
[7] Irawan B, Hindrasti NEK. Framework Literasi Kelautan Sebagai Acuan Pembelajaran Sains di Negara Maritim. *Pedagogi Hayati* 2018; 2: 14–23.
[8] Li M, Luo H, Zhou S, et al. State-of-the-art review of the flexibility and feasibility of emerging offshore and coastal ocean energy technologies in East and Southeast Asia. *Renewable and Sustainable Energy Reviews* 2022; 162: 112404.
[9] Aderinto T, Li H. Ocean wave energy converters: Status and challenges. *Energies (Basel)* 2018; 11: 1250.
[10] López I, Carballo R, Iglesias G. Site-specific wave energy conversion performance of an oscillating water column device. *Energy Convers Manag* 2019; 195: 457–465.
[11] Cheng Y, Li G, Ji C, et al. Fully nonlinear investigations on performance of an OWSC (oscillating wave surge converter) in 3D (three-dimensional) open water. *Energy* 2020; 210: 118526.
[12] Kofoed JP, Frigaard P, Friis-Madsen E, et al. Prototype testing of the wave energy converter wave dragon. *Renew Energy* 2006; 31: 181–189.
[13] Schubert BW, Robertson WSP, Cazzolato BS, et al. Linear and nonlinear hydrodynamic models for dynamics of a submerged point absorber wave energy converter. *Ocean Engineering* 2020; 197: 106828.
[14] Babarit A, Hals J, Muliawan MJ, et al. Numerical benchmarking study of a selection of wave energy converters. *Renew Energy* 2012; 41: 44–63.
[15] Renzi E, Doherty K, Henry A, et al. How does Oyster work? The simple interpretation of Oyster mathematics. *European Journal of Mechanics-B/Fluids* 2014; 47: 124–131.
[16] Whittaker T, Folley M. Nearshore oscillating wave surge converters and the development of Oyster. *Philosophical Transactions of the Royal Society A: Mathematical, Physical and Engineering Sciences* 2012; 370: 345–364.
[17] Anggara RA, Naufal RD, Ramadhani R, et al. Study of hydrodynamic characteristics in oscillating wave surge converter. *Jurnal Polimesin* 2024; 22: 158–164.
[18] Garcia-Teruel A, Forehand DIM. A review of geometry optimisation of wave energy converters. *Renewable and Sustainable Energy Reviews* 2021; 139: 110593.
[19] Henry A, Folley M, Whittaker T. A conceptual model of the hydrodynamics of an oscillating wave surge converter. *Renew Energy* 2018; 118: 965–972.
[20] Nguyen N, Davis J, Tom N, et al. Theoretical modeling of a bottom-raised oscillating surge wave energy converter structural loadings and power performances. *Applied Ocean Research* 2024; 149: 104031.
[21] Choiniere MA, Tom NM, Thiagarajan KP. Load shedding characteristics of an oscillating surge wave energy converter with variable geometry. *Ocean Engineering* 2019; 186: 105982.
[22] Wei Y, Rafiee A, Henry A, et al. Wave interaction with an oscillating wave surge converter, Part I: Viscous effects. *Ocean Engineering* 2015; 104: 185–203.

[23] Wei Y, Abadie T, Henry A, et al. Wave interaction with an oscillating wave surge converter. Part II: Slamming. *Ocean Engineering* 2016; 113: 319–334.
[24] Yu H-F, Zhang Y-L, Zheng S-M. Numerical study on the performance of a wave energy converter with three hinged bodies. *Renew Energy* 2016; 99: 1276–1286.
[25] Zhang DH. Research on the Key Technologies of Wave Energy Converter of Inverse Pendulum. *Zhejiang Univ*.
[26] Zhao HT. Hydrodynamic Research of A Bottom-Hinged Flap Wave Energy Convertor.
[27] Benites-Munoz D, Huang L, Thomas G. Optimal array arrangement of oscillating wave surge converters: An analysis based on three devices. *Renew Energy* 2024; 222: 119825.
[28] Liu Y, Mizutani N, Cho Y-H, et al. Performance enhancement of a bottom-hinged oscillating wave surge converter via resonant adjustment. *Renew Energy* 2022; 201: 624–635.
[29] Ahmed A, Yang L, Huang J, et al. Performance characterization and modeling of an oscillating surge wave energy converter. *Nonlinear Dyn* 2024; 112: 4007–4025.
[30] Lin Y, Pei F. Numerical study on bottom-hinged plate wave energy converter geometry design. *Ocean Engineering* 2022; 260: 112050.
[31] Roache PJ. Perspective: a method for uniform reporting of grid refinement studies.